# Two-photon ionization spectroscopy and all-electron *ab initio* study of LiCa

L. M. Russon, G. K. Rothschopf, M. D. Morse,[a)] A. I. Boldyrev, and Jack Simons
*Department of Chemistry, University of Utah, Salt Lake City, Utah 84112*

Resonant two-photon ionization spectra of LiCa have been obtained from a laser vaporization, supersonic expansion source. The ground state of the molecule is confirmed to be $X\ ^2\Sigma^+$. Three band systems have been observed near 15 282, 19 310, and 22 250 cm$^{-1}$ and the upper states have been assigned as $^2\Sigma^+$, $^2\Pi_r$, and, tentatively, $^2\Pi$. Bond lengths and vibrational frequencies are reported for $^7$Li$^{40}$Ca for the various states as $X\ ^2\Sigma^+$: $r_0 = 3.3796(11)$ Å, $\Delta G_{1/2} = 195.2$ cm$^{-1}$; $^2\Sigma^+$: $r_0 = 3.4275(47)$ Å, $\Delta G_{1/2} = 283.5$ cm$^{-1}$; $^2\Pi_r$: $r_e = 3.5451(36)$ Å, $\omega_e = 144.5$ cm$^{-1}$; and $^2\Pi$: $\omega_e = 178.53(5)$ cm$^{-1}$. The ionization energy was also measured to be 4.471(1) eV by observing the onset of one-photon ionization. Results of *ab initio* all-electron calculations on twelve low-lying states [$^2\Sigma^+(1)$, $^2\Sigma^+(2)$, $^2\Sigma^+(3)$, $^2\Sigma^+(4)$, $^4\Sigma^+(1)$, $^4\Sigma^-(1)$, $^2\Pi(1)$, $^2\Pi(2)$, $^2\Pi(3)$, $^2\Pi(4)$, $^4\Pi(1)$, and $^4\Pi(2)$] are also reported, along with results on the $X\ ^1\Sigma^+$ ground electronic state of LiCa$^+$. The dissociation energies of LiCa($X\ ^2\Sigma^+$) into Li($^2S$) + Ca($^1S$) and of LiCa$^+$ ($X\ ^1\Sigma^+$) into Li$^+$($^1S$) + Ca($^1S$) are calculated to be 0.24 and 1.20 eV respectively, and the vertical and adiabatic ionization energies of LiCa have been determined to be almost the same, 4.43 eV, at the quadratic configuration interaction, including singles and doubles with approximate triples and all correlated electrons [QCISD(T,FULL)] level of theory. © *1998 American Institute of Physics.* [S0021-9606(98)00240-2]

## I. INTRODUCTION

For the past several years work in the Morse laboratory has concentrated on the spectroscopy of diatomic transition metal molecules.[1] From this work we have gained a significant understanding of the bonding interactions between transition metals with open *d* subshells. More recently, a study of the bonding between transition metals and the main group metal aluminum was completed.[2] The object of that study was to probe the chemical bonding between *p*-block and *d*-block metals and to understand the role of the *d* orbitals in such interactions. Here we further extend those studies to alkali metals bonding to transition metals by investigating the spectroscopy of LiCa. While calcium is not a transition metal, it does have a stable $3d^0 4s^2$ ground configuration that is not readily promoted. It therefore serves as a useful model for the interactions of lithium with transition metals such as Mn and Zn which also have stable, not easily promoted, ground configurations of $3d^n 4s^2$. A related paper investigating the spectra of LiCu, a molecule that provides a useful model for the interaction of lithium with transition metals having accessible $3d^{n+1} 4s^1$ configurations, has already been published in this journal.[3]

Previous work on LiCa began in 1980 when a density functional calculation employing the local spin density approximation was published. That work resulted in estimates of $\omega_e'' = 190$ cm$^{-1}$, $r_e'' = 3.52$ Å, and $D_e = 0.27$ eV for the $^2\Sigma^+$ ground state.[4] A short time later Neumann *et al.* reported emission spectra from LiCa that were assigned as $A\ ^2\Pi \rightarrow X\ ^2\Sigma^+$ and $B\ ^2\Sigma^+ \rightarrow X\ ^2\Sigma^+$ transitions based on valence configuration interaction calculations.[5] These calcula-

tions, however, were in substantial disagreement with the density functional results, giving $\omega_e'' = 93.36$ cm$^{-1}$, $\omega_e'' x_e'' = 7.32$ cm$^{-1}$, $r_e'' = 3.883$ Å, and $D_e = 0.072$ eV for the $^2\Sigma^+$ ground state.[5] In 1983 Wu *et al.*, reported a bond energy of 0.84(9) eV based on a third law analysis of the vapors emanating from a Knudsen effusion cell, as studied by mass spectrometry.[6]

Most recently, a high-level *ab initio* study of LiCa has been reported by Allouche and Aubert-Frecon.[7] In that study nonempirical effective core potentials were employed with a large Gaussian basis set and extensive valence electron configuration interaction to estimate the potential curves of six $^2\Sigma^+$ states, five $^2\Pi$ states, two $^2\Delta$ states, two $^4\Sigma^+$ states, two $^4\Pi$ states, and one $^4\Delta$ state. The ground $X\ ^2\Sigma^+$ state was calculated to have $r_e = 3.296$ Å, $\omega_e = 196.13$ cm$^{-1}$, and a bond energy of $D_e = 0.292$ eV. Spectroscopic constants for eight excited electronic states were also reported.

It is clear that the closed shell nature of calcium, combined with the diffuse character of the Li $2s$ and Ca $4s$ orbitals, leads to a weak bond in this molecule. Nevertheless, the disparity of the reported results and the lack of detailed spectroscopic data on this molecule indicates a need for further experimental and theoretical work. In this paper we report the resonant two-photon ionization spectra of LiCa. Three band systems are observed, two of which are rotationally resolved and analyzed. In addition, extensive all-electron *ab initio* calculations on four $^2\Sigma^+$ states, one $^4\Sigma^+$ state, one $^4\Sigma^-$ state, four $^2\Pi$ states, and two $^4\Pi$ states are reported, along with a calculation of the $X\ ^1\Sigma^+$ state of LiCa$^+$. In Sec. II we describe the experimental methods employed in this study; the experimental results are presented in Sec. III. In Sec. IV the theoretical methods are described, while in Sec. V we provide theoretical results and their comparison to
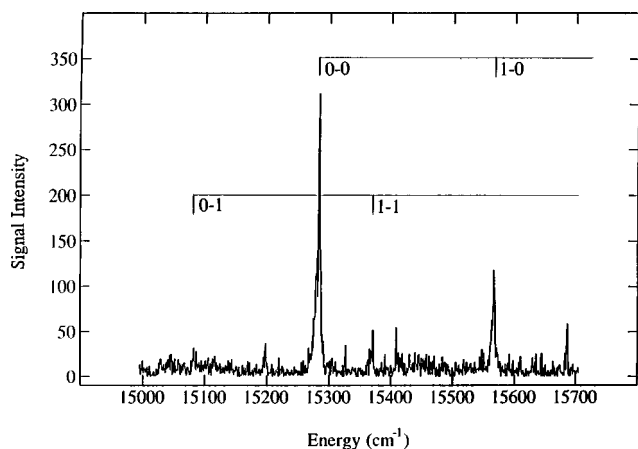
---

a)Electronic mail: morse@chemistry.chem.utah.edu

FIG. 1. A low resolution scan of the $[15.3]\,^2\Sigma^+ \leftarrow X\,^2\Sigma^+$ band system of $^7$Li $^{40}$Ca, collected using DCM dye laser radiation for excitation and the second harmonic of this radiation for photoionization. The identification of the 1–1 and 0–1 bands in this spectrum would have been impossible without the knowledge of $\Delta G''_{1/2}$ obtained from the other band systems.

previous theoretical calculations and to experiment. In Sec. VI we then conclude the paper with a summary of our most important findings.

## II. EXPERIMENT

The instrument used for this study was formerly used for ion photodissociation experiments, and has been described previously.[8] Modified ion acceleration optics were used in the present resonant two-photon ionization (R2PI) study of LiCa and in a previous R2PI study of LiCu,[3] but otherwise the instrument is similar to that previously described.

A metal alloy sample disk was formed by melting a 2:3 molar mixture of Ca:Li in an electric arc furnace under an argon atmosphere. The resulting alloy was machined flat on one side and mounted in a mechanism that rotates and translates the sample against a stainless steel vaporization block.[9] The output radiation from a KrF excimer laser (248 nm) was focused onto the metal disk and timed to fire during the peak density of a pulse of helium carrier gas (~120 psig backing pressure). The resulting metal plasma was entrained in the helium flow and swept down a 3 cm long, 2 mm diam clustering region before expanding supersonically from a conical diverging nozzle into a low-pressure chamber ($10^{-4}$ Torr). The metal cluster beam was roughly collimated by a 6.5 mm skimmer as it entered a differentially pumped ionization region. An excimer-pumped tunable dye laser was used to excite the LiCa molecules, and the excited molecules were subsequently photoionized by the absorption of a second photon of dye laser radiation, frequency doubled dye laser radiation, or by a portion of the 308 nm XeCl excimer radiation, which was picked off prior to pumping the dye laser.

Ions so produced were accelerated using a two-stage Wiley–McLaren ion extraction assembly.[10] Following a 300 cm drift tube the mass-separated ions were detected by a dual microchannel plate detector, the signal was preamplified, then digitized and signal averaged in a 386 DX-based personal computer.

Optical spectra were recorded by monitoring the mass channels of interest while scanning the dye laser frequency. Each data point was an average of 30 laser shots. Absolute wave number calibrations for the rotationally resolved spectra and the ionization threshold measurement were established by simultaneously recording the $I_2$ absorption spectrum and comparing to the $I_2$ atlas of Gerstenkorn and Luc.[11] For spectra outside of the range of the $I_2$ atlas the dye laser radiation was focused through a cell containing 500 psig of $H_2$ gas. The fundamental radiation was then used to excite the LiCa molecule while the Stokes shifted radiation was used to record the $I_2$ calibration spectrum. At this pressure a well-known Stokes shift of 4155.163 cm$^{-1}$ allows an absolute calibration to be made.[12] The excitation laser crossed the molecular beam at right angles, so no correction for the Doppler shift was required. For survey scans the dye laser was scanned rapidly; the scan rate was slowed down for rotationally resolved scans, and greater care was taken to avoid power broadening. In all cases the intrinsic linewidth of the dye laser was $\approx$0.07 cm$^{-1}$.

## III. RESULTS

Three band systems were observed over the range of 13 350–35 850 cm$^{-1}$. These consisted of a $^2\Sigma^+ \leftarrow X\,^2\Sigma^+$ system near 15 300 cm$^{-1}$: a $^2\Pi_r \leftarrow X\,^2\Sigma^+$ system near 19 300 cm$^{-1}$, and a third system, tentatively identified as $^2\Pi \leftarrow X\,^2\Sigma^+$, near 22 200 cm$^{-1}$. Each of these is discussed in turn below.

### A. The $[15.3]\,^2\Sigma^+ \leftarrow X\,^2\Sigma^+$ band system

Figure 1 displays a low-resolution scan over the $[15.3]\,^2\Sigma^+ \leftarrow X\,^2\Sigma^+$ system, where the designation $[15.3]\,^2\Sigma^+$ is used to indicate the $^2\Sigma^+$ state lying approximately 15 300 cm$^{-1}$ above the $v=0$ level of the ground state. Although somewhat unusual, this designation is preferable to the more conventional labeling of states as $A\,^2\Sigma^+$, $B\,^2\Pi$, etc., because it is never necessary to relabel the states if lower lying states are subsequently discovered. The two most intense features in Fig. 1 are assigned as the 0–0 and 1–0 bands, and much weaker features 199 cm$^{-1}$ to the red are assigned to the 0–1 and 1–1 vibrational hot bands. This ground state vibrational interval of $\Delta G''_{1/2} = 199$ cm$^{-1}$ is in reasonable agreement with theoretical predictions of $\Delta G''_{1/2} = 187.1$ cm$^{-1}$ (Ref. 7) and $\omega''_e = 204$ cm$^{-1}$ (see below). A more precise value is obtained from the $[19.3]\,^2\Pi_r \leftarrow X\,^2\Sigma^+$ and $[22.2]\,^2\Pi \leftarrow X\,^2\Sigma^+$ systems discussed below, because the vibrational hot bands were more prominent under the conditions of those scans, giving $\Delta G''_{1/2} = 195$ cm$^{-1}$. The wave numbers of the observed bands of this system and all other observed bands of the LiCa molecule are given in Table I.

A rotationally resolved scan over the 0–0 band is displayed in Fig. 2. The band consists of only P and R branches, and is weakly degraded toward the red, indicating a slight lengthening of the bond upon electronic excitation. This is consistent with the lack of observable $v'–0$ bands having $v' > 1$, which are expected to have weak Franck–Condon factors. The absence of a Q branch identifies the system as a $\Sigma \leftarrow \Sigma$ transition and the assignment of the ground state as

TABLE I. Vibronic bands of $^7$Li $^{40}$Ca.[a]

| System | Band | Energy[b] $(cm^{-1})$ | Isotope shift $(cm^{-1})$ | $B'$ $(cm^{-1})$[d,e] | $B''$ $(cm^{-1})$[d,e] |
|---|---|---|---|---|---|
| [15.3] $^2\Sigma^+ \leftarrow X\ ^2\Sigma^+$ | 0–0 | 15 282.1972[c] | −3.554 | 0.240 44(66) | 0.248 73(55) |
| | 1–0 | 15 565.65 | | | |
| | 0–1 | 15 082.15 | | | |
| | 1–1 | 15 367.62 | | | |
| [19.3] $^2\Pi_{1/2} \leftarrow X\ ^2\Sigma^+$ | 0–0 | 19 304.6193[c](−0.18) | 1.7058 | 0.219 61(50) | 0.246 59(39) |
| | 1–0 | 19 447.7583[c](0.30) | −8.2003 | 0.216 43(48) | 0.247 19(44) |
| | 2–0 | 19 589.6441[c](0.45) | −17.4251 | 0.213 69(51) | 0.246 83(44) |
| | 3–0 | 19 729.25(−0.75) | −28.2025 | | |
| | 4–0 | 19 870.06(0.19) | | | |
| | 1–1 | 19 252.31(−0.08) | | | |
| | 2–1 | 19 394.08(−0.04) | | | |
| | 3–1 | 19 534.92(−0.01) | | | |
| | 4–1 | 19 674.93(0.13) | | | |
| [19.3] $^2\Pi_{3/2} \leftarrow X\ ^2\Sigma^+$ | 0–0 | 19 317.7697[c](0.00) | 1.7355 | 0.228 05(25) | 0.247 40(23) |
| | 1–0 | 19 460.58(−0.39) | −7.6499 | | |
| | 2–0 | 19 602.7115[c](0.08) | | 0.226 66(98) | 0.247 66(68) |
| | 3–0 | 19 742.77(0.32) | −24.1367 | | |
| | 1–1 | 19 265.95(0.40) | | | |
| | 2–1 | 19 407.13(−0.08) | | | |
| | 3–1 | 19 546.71(−0.32) | | | |
| [22.2] $^2\Pi \leftarrow X\ ^2\Sigma^+$ | 0–0 | 22 249.46(0.03) | | | |
| | 1–0 | 22 420.82(−0.01) | | | |
| | 2–0 | 22 585.07(−0.02) | | | |
| | 0–1 | 22 054.17(−0.03) | | | |
| | 1–1 | 22 225.59(0.00) | | | |
| | 2–1 | 22 389.89(0.03) | | | |
| | 3–1 | 22 546.99(0.00) | | | |

[a]Energy and isotope shift given in units of $cm^{-1}$. The isotope shift is defined as $\nu_0(^7Li^{40}Ca) - \nu_0(^6Li^{40}Ca)$.
[b]Residuals to the fit to Eq. (3.2) shown in parentheses.
[c]The band origin measured in high resolution, calibrated against the $I_2$ atlas.
[d]Error limits $(1\sigma)$ are given in parentheses for fitted rotational constants.
[e]For the [19.3] $^2\Pi_{1/2} \leftarrow X\ ^2\Sigma^+$ and [19.3] $^2\Pi_{3/2} \leftarrow X\ ^2\Sigma^+$ systems $B_{eff}^{(1)}$ and $B_{eff}^{(2)}$ are given in this table.

$^2\Sigma^+$ further restricts the assignment to a $^2\Sigma^+ \leftarrow X\ ^2\Sigma^+$ system. No spin splitting is observed at the resolution obtained in Fig. 2, allowing the spectrum to be fit according to the simple expression[13]

$$\nu = \nu_0 + B'N'(N'+1) - B''N''(N''+1), \qquad (3.1)$$

resulting in $\nu_0 = 15\ 282.1972(67)$ $cm^{-1}$, $B_0' = 0.240\ 44(66)$ $cm^{-1}$, and $B_0'' = 0.248\ 73(55)$ $cm^{-1}$ for the most abundant isotopic modification, $^7Li^{40}Ca$. Converting to bond lengths, one obtains $r_0' = 3.4275(47)$ Å and $r_0'' = 3.3699(37)$ Å for the excited and ground state bond lengths, respectively. Rotational line positions for this and all other rotationally resolved bands are available from the Physics Auxiliary Publication Service[14] or the author (M.D.M.). All spectroscopic constants determined for this molecule are summarized in Table II.

The $^6Li^{40}Ca$ isotopic modification was similarly fit, giving $\nu_0 = 15\ 285.7508(56)$ $cm^{-1}$, $B_0' = 0.273\ 92(48)$ $cm^{-1}$, and $B_0'' = 0.283\ 89(58)$ $cm^{-1}$, which convert to $r_0' = 3.4313(30)$ Å and $r_0'' = 3.3705(34)$ Å. The agreement between the $r_0''$ and $r_0'$ values calculated for the two isotopic modifications provides additional confidence in the validity of the measurements.

## B. The [19.3] $^2\Pi_r \leftarrow X\ ^2\Sigma^+$ band system

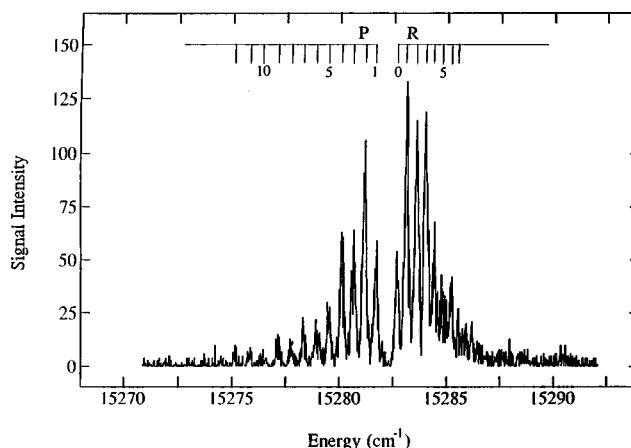Some 4000 $cm^{-1}$ to the blue a second band system, displayed in Fig. 3, was observed. Each band is split into two



FIG. 2. Rotationally resolved scan of the 0–0 band of the [15.3] $^2\Sigma^+ \leftarrow X\ ^2\Sigma^+$ band system of $^7Li^{40}Ca$. This band was excited using DCM dye laser radiation, and residual 308 nm XeCl excimer radiation was used for photoionization.

TABLE II. Spectroscopic constants of $^7\text{Li}^{40}\text{Ca}$.[a] IE(LiCa)=36 060(10) cm$^{-1}$=4.471(1) eV.

| State | $T_0$ (cm$^{-1}$) | $\omega_e$ (cm$^{-1}$) | $\omega_e x_e$ (cm$^{-1}$) | $B_0$ (cm$^{-1}$) | $r_0$ (Å) |
|---|---|---|---|---|---|
| $[22.2]\ ^2\Pi$ | 22 249.4 | 178.53(5) | 3.565(13) | | |
| $[19.3]\ ^2\Pi_{3/2}$ | 19 317.4697(59) | 144.98(75) | 0.851(171) | $B_e=0.224\ 74(38)\ \alpha_e=0.001\ 83(31)$ | $r_e=3.5451(30)$ |
| $[19.3]\ ^2\Pi_{1/2}$ | 19 304.6193(60) | 143.60(51) | 0.465(94) | | |
| $[15.3]\ ^2\Sigma^+$ | 15 282.1972(67) | $\Delta G_{1/2}=283.5$ | | 0.240 44(66) | 3.4275(47) |
| $X\ ^2\Sigma^+$ | 0.0 | $\Delta G_{1/2}=195.2(2)$ | | 0.247 34(16) | 3.3793(11) |

[a]Numbers in parentheses provide $1\sigma$ error limits.

spin–orbit sub-bands, implying a $^2\Pi \leftarrow X\ ^2\Sigma^+$ transition. The vibrational numbering is fairly evident from the Franck–Condon intensity pattern, and is confirmed by an analysis of the isotope shift between the $^6\text{Li}^{40}\text{Ca}$ and $^7\text{Li}^{40}\text{Ca}$ isotopic variants. The band positions, listed in Table I, were fit to the standard expression,[13]

$$\nu_{v'-v''}=T_0+\omega_e' v' - \omega_e' x_e'(v'^2+v') - \Delta G_{1/2}'' v'', \quad (3.2)$$

for the $\Omega=\frac{1}{2}$ and $\frac{3}{2}$ levels. We thus obtain for the $\Omega=\frac{1}{2}$ level: $T_0=19\ 304.8(4)$ cm$^{-1}$, $\omega_e'=143.6(5)$ cm$^{-1}$, and $\omega_e' x_e'=0.46(9)$ cm$^{-1}$ for $^7\text{Li}^{40}\text{Ca}$. For the $\Omega=\frac{3}{2}$ level of $^7\text{Li}^{40}\text{Ca}$, we obtain $T_0=19\ 317.4(4)$ cm$^{-1}$, $\omega_e'=145.3(7)$ cm$^{-1}$, and $\omega_e' x_e'=0.92(17)$ cm$^{-1}$. Improved values of these constants based on band origins obtained from rotationally resolved studies are listed below and in Table II. The fitted values of $\Delta G_{1/2}''$, independently obtained from the $^2\Pi_{1/2} \leftarrow X\ ^2\Sigma^+$ and $^2\Pi_{3/2} \leftarrow X\ ^2\Sigma^+$ subsystems, are 195.4(3) and 195.0(3) cm$^{-1}$, respectively. These are in excellent agreement with theoretical results.

A rotationally resolved scan over the 0–0 band is displayed in Fig. 4. The sub-bands clearly do not have the simple two-branch structure observed in the $[15.3]\ ^2\Sigma^+ \leftarrow X\ ^2\Sigma^+$ system. As expected from the observation of spin–orbit splitting, the complicated rotational structure implies a $^2\Pi(a) \leftarrow X\ ^2\Sigma^+$ system. Assuming negligible lambda doubling in the $^2\Pi$ state and an unresolvable spin–rotation interaction in the $X\ ^2\Sigma^+$ state, one may expect four branches in each subband. These are labeled $R_{11}$, $R_{12}+Q_{11}$, $Q_{12}+P_{11}$, and $P_{12}$ for the $^2\Pi_{1/2} \leftarrow X\ ^2\Sigma^+$ sub-band and $R_{21}$, $R_{22}+Q_{21}$, $Q_{22}+P_{21}$, and $P_{22}$ for the $^2\Pi_{3/2} \leftarrow X\ ^2\Sigma^+$ sub-band. Line positions are given by well-known formulas[13] in which the $^2\Pi_{1/2}$ and $^2\Pi_{3/2}$ levels have effective rotational constants $B_{\text{eff}}^{(1)}$ and $B_{\text{eff}}^{(2)}$, respectively, which are related to the true rotational constant, $B'$, according to

$$B_{\text{eff}}^{(i)}=B'(1\mp B'/A'). \quad (3.3)$$

In Eq. (3.3) the minus sign corresponds to $i=1$ and refers to the $^2\Pi_{1/2}$ level, the plus sign corresponds to $i=2$ and refers to the $^2\Pi_{3/2}$ level, and $B'$ and $A'$ are the rotational and spin–orbit constants of the $^2\Pi$ excited state, respectively.

The measured line positions were fit to the standard expressions,[13] providing $T_0^{(1)}(^2\Pi_{1/2})=19\ 304.6193(60)$ cm$^{-1}$, $T_0^{(2)}(^2\Pi_{3/2})=19\ 317.4697(59)$ cm$^{-1}$, $B_0''=0.247\ 19(20)$ cm$^{-1}$ $[r_0''=3.3803(14)\ \text{Å})]$, $B_{\text{eff}}^{(1)}=0.219\ 61(50)$ cm$^{-1}$, and $B_{\text{eff}}^{(2)}=0.228\ 05(25)$ cm$^{-1}$ for $^7\text{Li}^{40}\text{Ca}$. The spin–orbit constant, $A_v'$, is obtained directly from the fitted sub-band origins of the 0–0 and 2–0 $^2\Pi_{1/2} \leftarrow X\ ^2\Sigma^+$ and $^2\Pi_{3/2} \leftarrow X\ ^2\Sigma^+$ sub-bands, according to formula[15]

$$A_v'=T(^2\Pi_{3/2})-T(^2\Pi_{1/2})+2B_v'+3/4(B_{\text{eff}}^{(2)}-B_{\text{eff}}^{(1)}), \quad (3.4)$$

giving $A_0'=13.3044(84)$ cm$^{-1}$ and $A_2'=13.5175(181)$ cm$^{-1}$. From these results the true rotational constant of the $[19.3]\ ^2\Pi_r$ state is derived as $B_0'=[B_{\text{eff}}^{(1)}+B_{\text{eff}}^{(2)}]/2=0.223\ 83(28)$ cm$^{-1}$, giving $r_0'=3.5524(22)$ Å. As a test of this fit we note that the difference, $B_{\text{eff}}^{(2)}-B_{\text{eff}}^{(1)}$
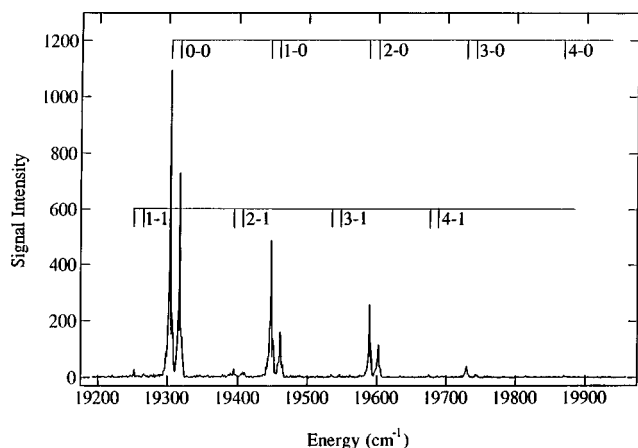


FIG. 3. Low resolution scan of the $[19.3]\ ^2\Pi_r \leftarrow X\ ^2\Sigma^+$ band system of $^7\text{Li}\ ^{40}\text{Ca}$, collected using coumarin 500 dye laser radiation for excitation and XeCl excimer radiation (308 nm) for photoionization.
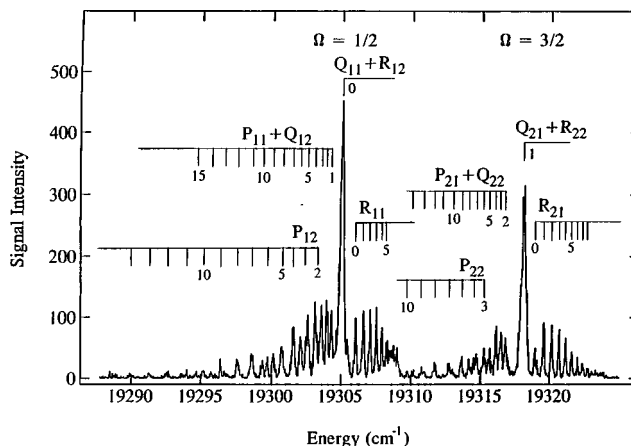


FIG. 4. Rotationally resolved scan of the 0–0 band of the $[19.3]\ ^2\Pi_r \leftarrow X\ ^2\Sigma^+$ band system of $^7\text{Li}\ ^{40}\text{Ca}$, collected using coumarin 500 dye laser radiation for excitation and XeCl excimer radiation (308 nm) for photoionization. Lines are labelled by the value of $N''$.
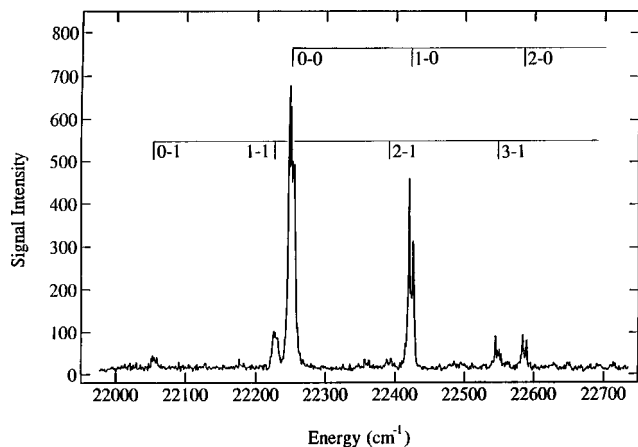
J. Chem. Phys., Vol. 109, No. 16, 22 October 1998

Russon et al.    6659



FIG. 5. Low resolution scan of the $[22.2]$ $^2\Pi \leftarrow X$ $^2\Sigma^+$ band system of $^7$Li $^{40}$Ca, collected using coumarin 440 dye laser radiation for excitation and XeCl excimer radiation (308 nm) for photoionization.



FIG. 6. Attempted high resolution scan of the 0–0 band of the $[22.2]$ $^2\Pi$ $\leftarrow X$ $^2\Sigma^+$ band system of $^7$Li $^{40}$Ca, using radiation sources as described in Fig. 5.

$(0.0084$ cm$^{-1})$, does indeed equal $2B_0'^2/A_0'$ (calculated as $0.0075$ cm$^{-1}$) to within experimental uncertainty, as required by Eq. (3.3).

The 0–0 and 2–0 bands of the $[19.3]$ $^2\Pi_r \leftarrow X$ $^2\Sigma^+$ system were fit in this manner, but the $^2\Pi_{3/2} \leftarrow X$ $^2\Sigma^+$ component of the 1–0 band displayed a perturbation in the upper state, which caused some rotational levels to disappear, presumably due to predissociation. As a result, only the $^2\Pi_{1/2} \leftarrow X$ $^2\Sigma^+$ sub-band of the 1–0 band was analyzed. Fitted effective rotational constants for the $^2\Pi_{1/2}$ component were obtained as $0.219\,61(50)(v'=0)$, $0.215\,86(38)(v'=1)$, and $0.213\,69(51)$ cm$^{-1}$ $(v'=2)$. For the $^2\Pi_{3/2}$ component effective rotational constants of $0.228\,05(25)(v'=0)$ and $0.226\,66(98)$ cm$^{-1}$ $(v'=2)$ were obtained for $^7$Li$^{40}$Ca. A fit of the $B_v'$ values for $v'=0,2$ then provides $B_e' = 0.224\,74(46)$ cm$^{-1}$ $\alpha_e=0.001\,83(33)$ cm$^{-1}$, $r_e' = 3.5451(36)$ Å, $A_0'=13.3044(84)$ cm$^{-1}$, and $A_2' = 13.5175(181)$ cm$^{-1}$ for the $[19.3]$ $^2\Pi_r$ state of LiCa.

## C. The $[22.2]$ $^2\Pi \leftarrow X$ $^2\Sigma^+$ band system

Figure 5 displays a low resolution scan over the $[22.2]$ $^2\Pi \leftarrow X$ $^2\Sigma^+$ band system, which is characterized by an intense band at $22\,249.5$ cm$^{-1}$, a fairly intense band at $22\,420.8$ cm$^{-1}$, and a weaker band at $22\,585.1$ cm$^{-1}$. These three bands clearly form a vibrational progression, which is accompanied by a series of weaker bands displaced approximately $195.2$ cm$^{-1}$ to the red. This interval has already been identified as $\Delta G_{1/2}''$, demonstrating that these are hot bands built off of the main progression. The fact that the redmost band of the main progression is the most intense identifies it as the origin band, and this establishes the vibrational assignment of the system. With this assignment the band positions were fit to Eq. (3.2), providing $T_0=22\,249.431(26)$ cm$^{-1}$, $\omega_e'=178.53(5)$ cm$^{-1}$, $\omega_e'x_e'=3.565(13)$ cm$^{-1}$, and $\Delta G_{1/2}''=195.23(3)$ cm$^{-1}$ for $^7$Li$^{40}$Ca.

A rotationally resolved scan over the 0–0 band, displayed in Fig. 6, reveals a complicated pattern of lines that is only partially resolved. Based on the intensity of the band system and the small spin–orbit parameters of lithium and calcium, it would seem that 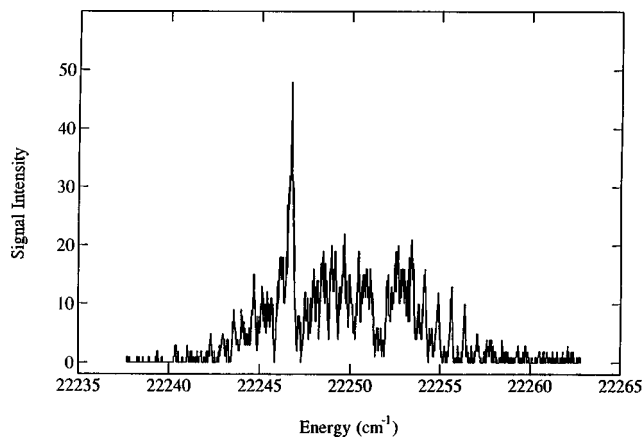the transition is fully allowed on the basis of $S$, $\Lambda$, and $\Sigma$. For transitions originating from an $X$ $^2\Sigma^+$ ground state, this excludes all candidates for the upper state except $^2\Sigma^+$ or $^2\Pi$. A $^2\Sigma^+ \leftarrow X$ $^2\Sigma^+$ system would only possess $R$ and $P$ branches (as found for the $[15.3]$ $^2\Sigma^+ \leftarrow X$ $^2\Sigma^+$ band system displayed in Fig. 2), a fact that is not consistent with the apparent complexity of the rotational structure in this system. On this basis, the band system is tentatively assigned as the $[22.2]$ $^2\Pi \leftarrow X$ $^2\Sigma^+$ system. The partially resolved scan over the 0–0 band also displays more structure than the three branches expected for a $^2\Pi(b) \leftarrow X$ $^2\Sigma^+$ system, but does not break out into clear-cut Hund's case (a) $^2\Pi_{1/2} \leftarrow X$ $^2\Sigma^+$ and $^2\Pi_{3/2} \leftarrow X$ $^2\Sigma^+$ sub-bands, as was found for the $[19.3]$ $^2\Pi_r \leftarrow X$ $^2\Sigma^+$ band system displayed in Fig. 4. It thus appears that the spin–orbit splitting of the $[22.2]$ $^2\Pi$ state is on the order of $A = 5$ cm$^{-1}$ or less, and that the $[22.2]$ $^2\Pi$ state may be intermediate between Hund's cases (a) and (b). Attempts to fit the resolved line positions were unsuccessful, but there is some evidence that the band is slightly red shaded, suggesting that the bond is lengthened slightly upon excitation.

## D. The LiCa ionization limit

Figure 7 displays a single-color scan over the ionization threshold of LiCa collected using frequency doubled dye laser radiation. Toward the low-frequency limit of this scan only a weak two-photon ionization background is evident. As one scans toward the blue, however, a weak rise in signal occurs near $35\,825$ cm$^{-1}$ followed by a sharp increase in signal at $36\,035$ cm$^{-1}$. Although no attempt was made to determine whether the relative intensities of these two features was dependent on experimental conditions, our favored interpretation is that the sharp increase in signal at $36\,035$ cm$^{-1}$ corresponds to the adiabatic ionization threshold, and the weaker rise in signal near $35\,825$ cm$^{-1}$ corresponds to ionization of vibrationally hot $(v''=1)$ LiCa molecules in the molecular beam. When corrected for field ionization effects, this leads to an adiabatic ionization energy of IE(LiCa) $=4.471(1)$ eV. This is slightly higher than the value calculated below (4.42 eV), but theoretical predictions tend to underestimate ionization energies because electron correla-
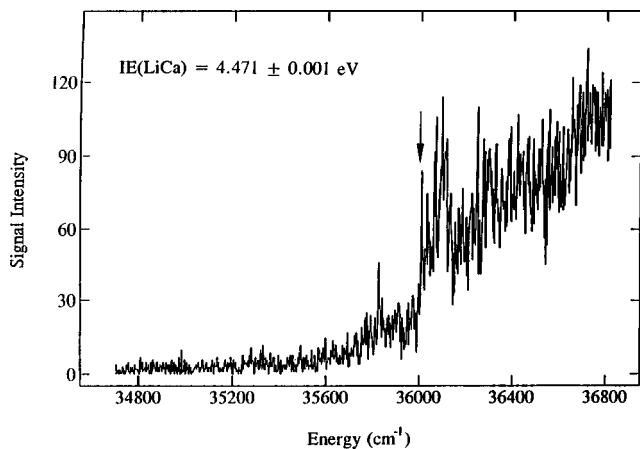
FIG. 7. Scan over the $^{7}\text{Li}\,^{40}\text{Ca}$ ionization threshold employing frequency doubled coumarin 540A dye laser radiation.

tion is more accurately treated in the cation than in the neutral. An alternative interpretation of the weak feature near 35 825 cm$^{-1}$ is that it corresponds to the adiabatic ionization threshold for the production of LiCa$^+$ in the $v^+$ vibrational level, while the sharper threshold at 36 035 cm$^{-1}$ is the threshold for producing the cation in the $v^+ + 1$ vibrational level. This interpretation would require a poor Franck–Condon factor for the 0–0 ionization process. Employing Morse potential approximations to the LiCa $X\,^2\Sigma^+$ and LiCa$^+$ $X\,^1\Sigma^+$ potential curves calculated below, however, a Franck–Condon factor for the 0–0 band of 0.8 is obtained. Furthermore, the separation between the two thresholds, although imperfectly defined, seems to be closer to the value of 195 cm$^{-1}$ measured for the $\Delta G'_{1/2}$ interval of the neutral ground state than it does to the value of $\omega_e = 239$ cm$^{-1}$ calculated below for the ground state of the cation. On this basis we assign the adiabatic ionization energy of LiCa as IE(LiCa)=4.471(1) eV.

## IV. THEORY

Two theoretical tools were used for calculations of the low-lying electronic states of LiCa and for the ground state of the LiCa$^+$ cation.

### A. MRCISD calculations

In the first method, the complete active space (CAS) self-consistent field (SCF) method was used to generate a basis of dominant electronic configurations for further multireference all single- and double-excitation configuration interaction calculations (CASSCF-MRCISD).[16] For these calculations we used large atomic natural orbital ANO basis sets for Li consisting of $(14s9p4d3f)$ elementary functions and $[7s6p4d3f]$ contracted functions,[17] and for Ca consisting of $(15s13p4d)$ elementary and $[9s7p2d]$ contracted functions.[18] Two active spaces have been used: $4a_1$, $2b_1$, $2b_2$, and $1a_2$ (4,2,2,1) and $6a_1$, $3b_1$, $3b_2$, and $1a_2$ (6,3,3,1) ($C_{2v}$ symmetry labeled), to check convergence toward the size of the active space. All three valence electrons were considered as active in the CASSCF calculations and all core orbitals were kept frozen in all of the CASSCF/MRCI calculations.

For the second (6,3,3,1) active-orbital space, we obtained 202 configurations for $^2\Sigma^+$ electronic states, 182 configurations for $^2\Pi$ states, 75 configurations for $^4\Sigma^-$ states, 65 configurations for $^4\Sigma^+$ states, and 73 configurations for $^4\Pi$ states to use in CASSCF expansions of the respective reference wave functions. All of these functions were then used in subsequent MRCI calculations in which the total number of configurations were 28 261 for $^2\Sigma^+$ states, 26 075 for $^2\Pi$ states, 11 851 for $^4\Sigma^-$ states, 13 618 for $^4\Sigma^+$ states, and 12 765 for $^4\Pi$ states. Attempts to examine $^2\Delta$ states were not successful because of a lack of convergence. The first, second, third, and fourth states of a given symmetry were calculated as the first, second, third, and fourth secular equation roots in the MRCI calculations.

The LiCa$^+$ cation was studied with the same atomic basis sets and using the following active-orbital space for CASSCF calculations: $6a_1$, $3b_1$, $3b_2$, and $1a_2$ (6,3,3,1). This leads to 34 configurations for the (6,3,3,1) orbital active space in the CASSCF expansion of the reference wave function and gives 1458 final configurations in the MRCI expansion.

Sixteen to twenty internuclear distances were calculated for each electronic state reported here. These MRCI energy data points were fit to an analytical form using cubic spline interpolation, after which the rovibrational Schrödinger equation was solved numerically (using Numerov's method) for one vibrational state at a time and for three rotational quantum numbers. All of these electronic and rovibrational calculations were performed using the MOLCAS-3 computer program.[19]

The calculated ionization energy of calcium (5.88 eV), and the Ca $^3P° \leftarrow ^1S$ and $^1P° \leftarrow ^1S$ excitation energies (1.68 and 3.03 eV, respectively) agree with the experimental values of 6.11, 1.89, and 2.93 eV,[20] respectively, to an accuracy of 0.2 eV.

### B. QCISD(T) calculations

In the second theoretical approach, the quadratic configuration interaction with single and double excitations and an approximate incorporation of triple excitations [QCISD(T)] method[21] was used with large atomic basis sets for geometry optimization of the lowest root in each symmetry [$^2\Sigma^+$, $^2\Pi$, $^4\Sigma^-$, $^4\Sigma^+$, and $^4\Pi$] for LiCa and for the ground state of LiCa$^+$. Again, attempts to calculate $^2\Delta$ states were not successful because of a lack of convergence. For lithium, the atomic orbital basis consisted of $(10s5p3d)$ elementary functions and $[6s5p3d]$ contracted functions, and for the Ca atom $(14s11p7d2f)$ elementary functions and $[8s7p6d2f]$ contracted functions. The $s$ functions of the Li basis set were constructed from the basis of Schäfer *et al.* $(10s)$[22] by contracting to $[6s]$ according to a $(5,1,1,1,1,1)$ scheme, with atomic coefficients in groups, and subsequently adding $5p$ and $3d$ elementary functions [$\alpha(p_1) = 3.3563$, $\alpha(p_2) = 1.1188$, $\alpha(p_3) = 0.3729$, $\alpha(p_4) = 0.1243$, $\alpha(p_5) = 0.0414$, $\alpha(d_1) = 4.22$, $\alpha(d_2) = 1.41$, and $\alpha(d_3) = 0.47$]. The Ca basis set was built from that of Schäfer *et al.* $(14s11p/8s7p)$[22] by adding $7d$ and $2f$ elementary functions contracted to $6d$ and $2f$ functions, as recommended by Bauschlicher *et al.*[23] The core orbitals were kept frozen in all

QCISD(T) calculations, except in the calculations for the ground electronic state of LiCa, where all electrons were included in the correlation. These calculations were performed using the GAUSSIAN-92 program.[24]

The calculated ionization energies IE(Li)=5.34 eV, IE(Ca)=5.89 eV, and excitation energy $\Delta E(Ca\,^3P^\circ \leftarrow {}^1S)$ =1.67 eV again agree with the experimental values[20] IE(Li) =5.39 eV, IE(Ca)=6.11 eV, and $\Delta E(Ca\,^3P^\circ \leftarrow {}^1S)$ =1.89 eV to within 0.2 eV. Because the quality of the ionization and excitation energy results for Ca and Li are virtually the same for the MRCI and QCISD(T) methods, we feel comfortable in proceeding to use both approaches for LiCa and LiCa$^+$.

## V. THEORETICAL RESULTS AND COMPARISON WITH EXPERIMENT

### A. Molecular orbitals of LiCa

The lowest *valence* $1\sigma$ molecular orbital is composed of $2s_{Li}$, $2p\sigma_{Li}$, and $4s_{Ca}$ atomic orbitals, with bonding (in-phase) interactions between $2s_{Li}$ and $4s_{Ca}$ as well as between $2p\sigma_{Li}$ and $4s_{Ca}$. The $2\sigma$ molecular orbital is composed of $2s_{Li}$, $4s_{Ca}$, and $4p\sigma_{Ca}$, with bonding interactions between $2s_{Li}$ and $4p\sigma_{Ca}$ and antibonding interactions between $2s_{Li}$ and $4s_{Ca}$. Occupation of this orbital causes the internuclear separation to increase. The $3\sigma$ orbital is antibonding with respect to the $2s_{Li}-4p\sigma_{Ca}$ interaction, but bonding with respect to the $2p\sigma_{Li}-4p\sigma_{Ca}$ interaction. The $1\pi$ molecular orbital is bonding with respect to the $2p\pi_{Li}-4p\pi_{Ca}$ interaction and the $2\pi$ orbital is antibonding with respect to the same interaction.

The molecular constants obtained at the CASSCF-MRCI level with the larger (6,3,3,1) active-orbital space and at the QCISD(T) level of theory, for the 12 electronic states of LiCa and for the ground state of LiCa$^+$, are presented in Table III.

### B. $^2\Sigma^+$ states of LiCa

The ground state is of $^2\Sigma^+$ symmetry and has a $1\sigma^2 2\sigma^1$ dominant electronic configuration ($C_{HF}=0.9374$). None of the remaining 28 260 configuration state functions (CSFs) has an expansion amplitude larger than 0.15. The small influence of the secondary configurations may be seen in the natural occupation numbers of the lowest valence molecular orbitals: $1\sigma^{1.82} 2\sigma^{0.97} 3\sigma^{0.05} 4\sigma^{0.02} 1\pi_x^{0.05} 1\pi_y^{0.05} 2\pi_x^{0.02} 2\pi_y^{0.02}$.

The ground electronic state of LiCa correlates with the atomic ground states of Li($^2S$) and Ca($^1S$). The charge distribution in the ground $X\,^2\Sigma^+$ state has significant ionic character with Mulliken atomic charges of Li$^{-0.54}$Ca$^{+0.54}$, as obtained from our MRCI wave function. The LiCa($X\,^2\Sigma^+$) state is weakly bound with $D_e=0.27$ eV at the CASSCF/ MRCI and QCISD(T) levels of theory, and is very flat with a harmonic frequency of *ca.* 200 cm$^{-1}$.

It is known that ignoring the core–valence correlation may substantially affect computed bond lengths in diatomic molecules such as $K_2$,[25] where the equilibrium bond length is 0.39 Å longer when core–valence correlations are not taken into account. To estimate the influence of the core–valence correlation on the ground electronic state of LiCa we

performed QCISD(T,FULL) calculations, where *all* electrons were included in the correlation, and we found $D_e$ =0.27 eV, $\omega_e=194$ cm$^{-1}$, and $r_e=3.410$ Å at the QCISD(T) level of theory and $D_e=0.24$ eV, $\omega_e$ =185 cm$^{-1}$, and $r_e=3.395$ Å at the QCISD(T,FULL) level of theory. We therefore believe that the core–valence correlation will not substantially affect our results for excited states, where the core electrons were not included in the correlation treatment.

The first $^2\Sigma^+$ symmetry *excited* state $[^2\Sigma^+(2)]$ has two dominant electronic configurations $1\sigma^2 2\sigma^0 3\sigma^1$ ($C$ $=-0.7092$) and $1\sigma^1 2\sigma^2 3\sigma^0$ ($C=0.5358$) in the MRCI expansion, and arises from the $X\,^2\Sigma^+$ ground state by (partial) promotion of an electron from the $1\sigma$ and $2\sigma$ orbitals into the $3\sigma$ orbital. This is clearly seen in the natural orbital occupation numbers of the lowest valence molecular orbitals: $1\sigma^{1.52} 2\sigma^{0.68} 3\sigma^{0.66} 4\sigma^{0.02} 1\pi_x^{0.05} 1\pi_y^{0.05} 2\pi_x^{0.01} 2\pi_y^{0.01}$. The $^2\Sigma^+(2)$ electronic state has an ionic character similar to that of the ground state, with natural atomic charges of Li$^{-0.56}$Ca$^{+0.56}$, as obtained from the MRCI wave function. According to our best calculations, the vertical excitation $[^2\Sigma^+(2)\leftarrow X\,^2\Sigma^+]$ energy is 1.16 eV and $T_e[^2\Sigma^+(2) \leftarrow X\,^2\Sigma^+]=1.13$ eV, both at the CASSCF-MRCI level of theory.

We did not expect our calculations for the third $^2\Sigma^+(3)$ and the fourth $^2\Sigma^+(4)$ roots to be of high quality because of known limitations of the CASSCF-MRCI method on excited states of the same symmetry. We attempted to increase the active-orbital space beyond the (6,3,3,1) level to improve the calculations, but convergence difficulties prohibited this. Nevertheless, we present results on these states in Table III to help identification of the experimentally observed transitions. The vertical excitation energies are 1.76 eV $[^2\Sigma^+(3)]$ and 2.42 eV $[^2\Sigma^+(4)]$, and the adiabatic excitation energies are $T_e[^2\Sigma^+(3)]=1.70$ eV and $T_e[^2\Sigma^+(4)]=2.42$ eV, all at the CASSCF-MRCI level of theory. A better description of these roots will lower these excitation energies. Neither state is adequately represented by one electronic configuration; instead, four configurations have coefficients larger than 0.20: $1\sigma^1 2\sigma^2(0.6135)$, $1\sigma^2 4\sigma^1(-0.3938)$, $1\sigma^2 3\sigma^1(0.3660)$, $1\sigma^\alpha 2\sigma^\beta 3\sigma^\alpha(-0.2241)$ for the $^2\Sigma^+(3)$ state and six configurations have coefficients larger than 0.20: $1\sigma^2 4\sigma^1(0.5734)$, $1\sigma^\alpha 2\sigma^\alpha 3\sigma^\beta(0.2967)$, $1\sigma^1 2\sigma^2(-0.2949)$, $1\sigma^2 12\sigma^1(-0.2375)$, $1\sigma^1 3\sigma^2(0.2311)$, and $1\sigma^2 8\sigma^1(-0.2294)$ for the $^2\Sigma^+(4)$ state.

### C. $^2\Pi$ states of LiCa

The lowest $^2\Pi(1)$ state has a $1\sigma^2 1\pi^1$ dominant electronic configuration ($C_{HF}=0.9246$) in the MRCI expansion and is the first excited state of LiCa. From the total of 26 075 CSFs, only one other configuration has a coefficient larger than 0.20: $1\sigma^0 2\sigma^2 1\pi_x^1(-0.2051)$. The vertical $^2\Pi(1)$ $\leftarrow X\,^2\Sigma^+$ excitation energy is computed to be 0.83 eV and $T_e(^2\Pi(1)\leftarrow X^2\Sigma^+)=0.75$ eV. The $^2\Pi(1)$ state has significant ionic character with natural atomic charges Li$^{-0.59}$Ca$^{+0.59}$, as obtained from the MRCI wave function. Because the $1\pi$-MO is bonding, electron transfer from the $2\sigma$-MO into the $1\pi$-MO during the $^2\Pi(1)\leftarrow X\,^2\Sigma^+$ excitation leads to a decrease in the equilibrium bond length of

TABLE III. Comparisons between theoretical calculations and experiment for $^7$Li $^{40}$Ca.

| State | Property | QCISD(T)[a] | CASSCF-MRCISD[a] | Pseudopotential-CIPSI[b] | Experiment[a] | Separated atom limit[c] |
|---|---|---|---|---|---|---|
| $X\ ^2\Sigma^+(1)$ | $r_e$ (Å) | 3.410 | 3.400 | 3.296($r_0 = 3.39$)[d] | $r_0 = 3.3796(11)$ | Li $2s^1$, $^2S$ |
| $1\sigma^2 2\sigma^1$ | $\omega_e$ (cm$^{-1}$) | 194 | 204 | 195.28($\Delta G_{1/2} = 187.1$)[d] | $\Delta G_{1/2} = 195.2$ | + |
| | $D_e$ (eV) | 0.27 | 0.27 | 0.292 | 0.84[e] | Ca $4s^2$, $^1S$ |
| | | | | | | 0.00 cm$^{-1}$ |
| $^2\Pi(1)$ | $r_e$ (Å) | 3.015 | 3.052 | 2.862 | | Li $2p^1$, $^2P°$ |
| $1\sigma^2 1\pi^1$ | $\omega_e$ (cm$^{-1}$) | 280 | 286 | 306.34[d] | | + |
| | $T_e$ (cm$^{-1}$) | 6355 | 6028 | 5464 | | Ca $4s^2$, $^1S$ |
| | | | | | | 14 903.83 cm$^{-1}$ |
| $^2\Sigma^+(2)$ | $r_e$ (Å) | | 3.634 | 3.423 | | Li $2p^1$, $^2P°$ |
| | $\omega_e$ (cm$^{-1}$) | | 192 | 219.60[d] | | + |
| | $T_e$ (cm$^{-1}$) | | 9138 | 9554 | | Ca $4s^2$, $^1S$ |
| | | | | | | 14 903.83 cm$^{-1}$ |
| $^4\Pi(1)$ | $r_e$ (Å) | 3.361 | 3.394 | 3.105 | | Li $2s^1$, $^2S$ |
| $1\sigma^1 2\sigma^1 1\pi^1$ | $\omega_e$ (cm$^{-1}$) | 201 | 201 | 242.19[d] | | + |
| | $T_e$ (cm$^{-1}$) | 12 390 | 12 815 | 13 169 | | Ca $4s^1 4p^1$, $^3P°$ |
| | | | | | | 15 263.10 cm$^{-1}$ |
| $^2\Sigma^+(3)$ | $r_e$ (Å) | | (3.774)[f] | Omitted | | Li $2s^1$, $^2S$ |
| | $\omega_e$ (cm$^{-1}$) | | (171)[f] | from | | + |
| | $T_e$ (cm$^{-1}$) | | (13 704)[f] | table | | Ca $4s^1 4p^1$, $^3P°$ |
| | | | | | | 15 263.10 cm$^{-1}$ |
| $^2\Pi(2)$ | $r_e$ (Å) | | 3.346 | 2.990 | | Li $2s^1$, $^2S$ |
| | $\omega_e$ (cm$^{-1}$) | | 206 | 275.41[d] | | + |
| | $T_e$ (cm$^{-1}$) | | 13 825 | 12 016 | | Ca $4s^1 4p^1$, $^3P°$ |
| | | | | | | 15 263.10 cm$^{-1}$ |
| $^2\Sigma^+(4)$ | $r_e$ (Å) | | (3.365)[f] | 3.310($r_0 = 3.44$)[d] | $r_0 = 3.3699(37)$ | Li $2s^1$, $^2S$ |
| | $\omega_e$ (cm$^{-1}$) | | (242)[f] | 290.46($\Delta G_{1/2} = 285.01$)[d] | $\Delta G_{1/2} = 284.5$ | + |
| | $T_e$ (cm$^{-1}$) | | (19 505)[f] | 14 708 | 15 237.6 | Ca $4s^1 3d^1$, $^3D$ |
| | | | | | | 20 356.61 cm$^{-1}$ |
| $^2\Delta(1)$ | $r_e$ (Å) | | | 2.968 | | Li $2s^1$, $^2S$ |
| | $\omega_e$ (cm$^{-1}$) | | | 275.73[d] | | + |
| | $T_e$ (cm$^{-1}$) | | | 14 754 | | Ca $4s^1 3d^1$, $^3D$ |
| | | | | | | 20 356.61 cm$^{-1}$ |
| $^4\Sigma^+(1)$ | $r_e$ (Å) | 5.600 | 4.708 | | | Li $2s^1$, $^2S$ |
| $1\sigma^1 2\sigma^1 3\sigma^1$ | $T_e$ (cm$^{-1}$) | 15 505 | 15 915 | | | + |
| | | | | | | Ca $4s^1 4p^1$, $^3P°$ |
| | | | | | | 15 263.10 cm$^{-1}$ |
| $^4\Sigma^-$ | $r_e$ (Å) | 2.851 | 2.925 | 2.636 | | Li $2p^1$, $^2P°$ |
| $1\sigma^1 2\sigma^0 1\pi^2$ | $\omega_e$ (cm$^{-1}$) | 288 | 286 | 317.17[d] | | + |
| | $T_e$ (cm$^{-1}$) | 18 426 | 19 196 | 18 546 | | Ca $4s^1 4p^1$, $^3P°$ |
| | | | | | | 30 166.93 cm$^{-1}$ |
| $^2\Pi(3)$ | $r_e$ (Å) | | (3.507)[f] | 3.456 | 3.5451(36) | Li $2s^1$, $^2S$ |
| | $\omega_e$ (cm$^{-1}$) | | (169)[f] | 149.48[d] | 144.5 | + |
| | $T_e$ (cm$^{-1}$) | | (22 545)[f] | 19 122 | 19 285.8 | Ca $4s^1 3d^1$, $^3D$ |
| | | | | | | 20 356.61 cm$^{-1}$ |
| $^4\Pi(2)$ | $r_e$ (Å) | | 3.871 | | | Li $2s^1$, $^2S$ |
| | $\omega_e$ (cm$^{-1}$) | | 174 | | | + |
| | $T_e$ (cm$^{-1}$) | | 22 810 | | | Ca $4s^1 3d^1$, $^3D$ |
| | | | | | | 20 356.61 cm$^{-1}$ |
| $^2\Pi(4)$ | $r_e$ (Å) | | (3.410)[f] | | | Li $2s^1$, $^2S$ |
| | $\omega_e$ (cm$^{-1}$) | | (148)[f] | | 178.5 | + |
| | $T_e$ (cm$^{-1}$) | | (23 693)[f] | | | Ca $4s^1 3d^1$, $^1D$ |
| | | | | | 22 257.8 | 21 849.61 cm$^{-1}$ |
| LiCa$^+$ | $r_e$ (Å) | 3.320 | 3.319 | | | Li$^+$ $1s^2$, $^1S$ |
| $X\ ^1\Sigma^+$ | $\omega_e$ (cm$^{-1}$) | 239 | 239 | | | + |
| $1\sigma^2$ | IE (cm$^{-1}$) | 35 336 | 35 642 | | | Ca $4s^2$, $^1S$ |
| | | | | | 36 060±10 | 43 487.19 cm$^{-1}$ |

[a]This work.

[b]Reference 7.

[c]Deduced from the atomic energy levels listed in Ref. 21.

[d]In examining Table 2 of Ref. 7, it became clear that the reduced mass employed in the conversion of $r_e$ to the rotational constant $B_e$ did not correspond to any particular isotopic combination of LiCa, but instead used the atomic weights of Li and Ca, which are averages of the atomic masses for the various isotopes. Presumably the vibrational parameters $\omega_e$ and $\omega_e x_e$ were also calculated in Ref. 7 for this isotopically averaged mass combination as well. Using the well-known dependence of these parameters on reduced mass, in this table we have converted these calculated vibrational constants to those appropriate for the most abundant isotopic species, $^7$Li$^{40}$Ca.

[e]Reference 6.

[f]Parentheses indicate that these theoretical results are not expected to be of high quality. A better treatment of these roots will cause $T_e$ to decrease.

J. Chem. Phys., Vol. 109, No. 16, 22 October 1998

Russon *et al.* 6663

0.35 Å. The potential energy curve of the $^2\Pi(1)$ state is steeper than that of the ground state and has a harmonic frequency of $\omega_e = 286$ cm$^{-1}$. The molecular parameters calculated for this state using the CASSCF-MRCI methods are in excellent agreement and also agree with the results of the QCISD(T) method.

The second excited state of $^2\Pi$ symmetry $[^2\Pi(2)]$ again has two dominant electronic configurations, $1\sigma^2 2\pi^1 (C = +0.7277)$ and $1\sigma^\alpha 2\sigma^\alpha 2\pi^\beta (C = -0.4477)$, in the MRCI expansion. From the total of 26 075 CSFs, only one other configuration has a coefficient larger than 0.20: $1\sigma^\alpha 2\sigma^\beta 2\pi_x^\alpha (-0.2852)$. The $^2\Pi(2)$ electronic state also has significant ionic character with natural atomic charges of Li$^{-0.55}$Ca$^{+0.55}$, as obtained from the MRCI wave function. According to our best calculations, the vertical excitation $[^2\Pi(2) \leftarrow X\,^2\Sigma^+]$ energy is 1.72 eV and $T_e[^2\Pi(2) \leftarrow X\,^2\Sigma^+] = 1.71$ eV, at the CASSCF-MRCI level of theory.

Again, we did not expect our calculations for the third $^2\Pi(3)$ and the fourth $^2\Pi(4)$ roots to be of high quality. However, we present these results in Table III to help with the identification of the experimentally observed transitions. The adiabatic excitation energies are $T_e[^2\Pi(3) \leftarrow X\,^2\Sigma^+] = 2.80$ eV and $T_e[^2\Pi(4) \leftarrow X\,^2\Sigma^+] = 2.94$ eV at the CASSCF-MRCI level of theory, which are the same as the vertical excitation energies. Again, a better description of these roots will cause the excitation energies to be lowered. Neither state is well represented by a single configuration. Instead, four configurations have coefficients larger than 0.20 for the $^2\Pi(3)$ state: $1\sigma^\alpha 2\sigma^\alpha 2\pi^\beta (0.6155)$, $1\sigma^2 5\pi^1 (-0.3797)$, $1\sigma^2 3\pi^1 (-0.2942)$, $1\sigma^2 1\pi^1 (-0.2774)$, and five configurations have coefficients larger than 0.20 for the $^2\Pi(4)$ state: $1\sigma^2 4\pi^1 (-0.4862)$, $1\sigma^2 2\pi^1 (0.4368)$, $1\sigma^\alpha 6\sigma^\beta 1\pi^\alpha (0.2549)$, $1\sigma^2 7\pi^1 (-0.2393)$, and $1\sigma^\alpha 6\sigma^\alpha 1\pi^\beta (0.2124)$.

### D. $^4\Pi$ states of LiCa

The lowest $^4\Pi$ state $[^4\Pi(1)]$ has a $1\sigma^1 2\sigma^1 1\pi_x^1$ dominant electronic configuration ($C_{HF} = -0.9773$) in the MRCI expansion. The vertical and adiabatic $^4\Pi(1) \leftarrow X\,^2\Sigma^+$ excitation energies are almost the same, 1.59 eV. The $^4\Pi(1)$ state has some ionic character, with Mulliken atomic charges of Li$^{-0.44}$Ca$^{+0.44}$, as obtained from the MRCI wave function. Because both the $1\sigma$- and $1\pi$-MOs have bonding character, promoting an electron from the $1\sigma$- into the $1\pi$-MO does not strongly affect the equilibrium bond length.

The second excited state of $^4\Pi$ symmetry $[^4\Pi(2)]$, calculated as the second root of the secular problem, has two dominant electronic configurations: $1\sigma^1 2\sigma^1 1\pi^0 2\pi^1 (C = +0.8155)$ and $1\sigma^1 2\sigma^0 3\sigma^1 1\pi^1 (C = +0.4098)$ in the MRCI expansion. All other configurations have expansion coefficients less than 0.15. The $^4\Pi(2)$ electronic state has substantial ionic character with natural atomic charges of Li$^{-0.59}$Ca$^{+0.59}$, as obtained from the MRCISD wave function. The vertical excitation energy of $^4\Pi(2) \leftarrow X\,^2\Sigma^+$ is 2.92 eV and $T_e[^4\Pi(2) \leftarrow X\,^2\Sigma^+]$ is 2.83 eV.

### E. $^4\Sigma^-$ state of LiCa

The lowest $^4\Sigma^-$ state has a $1\sigma^1 1\pi^2$ dominant electron configuration ($C_{HF} = 0.9725$) in the MRCI expansion. The

vertical $^4\Sigma^-(1) \leftarrow X\,^2\Sigma^+$ excitation energy is computed to be 2.53 eV and $T_e[^4\Sigma^-(1) \leftarrow X\,^2\Sigma^+] = 2.38$ eV. The $^4\Sigma^-(1)$ state has less ionic character than the other states calculated, with natural atomic charges of Li$^{-0.29}$Ca$^{+0.29}$ obtained from the MRCI wave function. The transfer of two electrons, one from the $1\sigma$-MO into the $1\pi$-MO and another from the $2\sigma$-MO into the $1\pi$-MO during the $^4\Sigma^-(1) \leftarrow X\,^2\Sigma^+$ excitation, leads to a decrease in equilibrium bond length of 0.47 Å. Again, we find excellent agreement for the molecular parameters of this state at the CASSCF-MRCI and QCISD(T) levels of theory.

### F. $^4\Sigma^+$ state of LiCa

The lowest $^4\Sigma^+$ state has a $1\sigma^1 2\sigma^1 3\sigma^1$ dominant electronic configuration ($C_{HF} = 0.9863$) in the MRCI expansion, and has a very weak van der Waals minimum with $r_e = 4.708$ Å, a vertical excitation energy $[^4\Sigma^+(1) \leftarrow X\,^2\Sigma^+] = 2.18$ eV, $T_e[^4\Sigma^+(1) \leftarrow X\,^2\Sigma^+] = 1.97$ eV, and $D_e = 0.056$ eV at the CASSCF/MRCI level of theory, and $r_e = 5.600$ Å, a vertical excitation energy $[^4\Sigma^+(1) \leftarrow X\,^2\Sigma^+]$ of 2.13 eV, $T_e[^4\Sigma^+(1) \leftarrow X\,^2\Sigma^+] = 1.92$ eV, and $D_e = 0.022$ eV at the QCISD(T) level of theory. Agreement between the CASSCF/MRCI and QCISD(T) data is rather poor for this state compared to the other cases, because the potential energy curve is very shallow, and thus differences in basis sets and in methods of treatment of the correlation energy affect the computed molecular constants appreciably.

### G. $X\,^1\Sigma^+$ state of LiCa$^+$ and ionization potential of LiCa

The $^1\Sigma^+$ electronic state of LiCa$^+$ arising from the $1\sigma^2$ electronic configuration, is expected to be the ground electronic state. The $1\sigma^2$ CSF was found to be the dominant electronic configuration ($C_{HF} = 0.9573$) in the MRCI expansion. From the total of 1458 CSFs, only one other configuration has a coefficient larger than 0.20: $1\sigma^0 2\sigma^2 (-0.2096)$. This electronic state correlates with the ground electronic states of the Li$^+(^1S)$ cation and the Ca($^1S$) atom. The vertical and adiabatic ionization potentials are predicted to be the same: 4.43 eV at the CASSCF/MRCI and 4.38 eV at the QCISD(T) levels of theory, and both are in excellent agreement with the experimental IE(LiCa) = 4.471 ± 0.001 eV. Moreover, the 0.04 eV difference between our computed IE(LiCa) and the experimental value is in line with the 0.05 eV difference between our IE(Li) and the experimental data. Although our error in IE(Ca) is larger (0.2 eV), for the state of LiCa being considered, the quality of our computed IE is likely more related to IE(Li) than to IE(Ca) because the molecular ion state has more Li$^+$Ca than LiCa$^+$ character.

To estimate the influence of the core–valence correlation on the dissociation energy of the ground electronic state of LiCa$^+$ and on the ionization energy of LiCa, we performed QCISD(T,FULL) calculations of LiCa$^+$, where all electrons were included in correlation at the QCISD(T) optimal geometry. The values of $D_e(\text{LiCa}^+) = 1.24$ eV and IE(LiCa) = 4.38 eV obtained at the QCISD(T) level of theory compare well with $D_e(\text{LiCa}^+) = 1.20$ eV and IE(LiCa) = 4.43 eV, obtained at the QCISD(T,FULL) level of theory. Hence, the influence

from the core–valence correlation is rather small. The bond length in LiCa$^+$ is *ca.* 0.1 Å shorter than in the ground state of LiCa, because an electron is removed from the partially antibonding $2\sigma$-MO. The LiCa$^+$ cation is found to be more strongly bound than the neutral LiCa molecule; the bond dissociation energy for breaking LiCa$^+$ into Li$^+$+Ca is 1.20 eV using the QCISD(T,FULL) computational method. For the ground state of LiCa$^+$ we have very good agreement between all theoretical methods (Table III).

## H. Comparisons to experiment and to previous calculations

Table III also provides comparisons between the eight electronic states of LiCa and LiCa$^+$ calculated in this study, the nine electronic states tabulated in the previous study by Allouche and Aubert-Frécon,[7] and the five electronic states (four for LiCa and one for LiCa$^+$) for which some experimental information is available. Quite unfortunately, it appears that all of the excited states of neutral LiCa calculated to high quality in the present study lie below the excited states that have been experimentally probed. Nevertheless, it appears that the [15.3] $^2\Sigma^+$ state is the $^2\Sigma^+(4)$ state, the [19.3] $^2\Pi_r$ state is the $^2\Pi(3)$ state, and the [22.2] $^2\Pi$ state is the $^2\Pi(4)$ state.

Both the present calculations and the previous study by Allouche and Aubert-Frécon[7] are in reasonable agreement with the experiment for the bond length and vibrational frequency of the ground $X$ $^2\Sigma^+$ state. The close agreement between the bond energies predicted by these two studies, particularly given the quality of the basis sets employed and the extent of the configuration interaction included, demonstrates that the third law value of the bond energy reported by Wu *et al.*, $D_0 = 0.84(9)$ eV,[6] is seriously in error.

The remaining excited states that have been calculated both in the present study and by Allouche and Aubert-Frécon are the $^2\Pi(1)$, $^2\Sigma^+(2)$, $^4\Pi(1)$, $^2\Pi(2)$, $^2\Sigma^+(4)$, $^4\Sigma^-(1)$, and $^2\Pi(3)$. Both studies predict the $^2\Pi(1)$ state to lie quite low in energy, with a much shorter bond length and substantially higher vibrational frequency than the ground state. This state lies roughly 13 000 cm$^{-1}$ below the [19.3] $^2\Pi$ state, which is experimentally observed. Likewise, both studies calculate the $^2\Pi(2)$ state to lie more than 5000 cm$^{-1}$ below the [19.3] $^2\Pi$ state. On this basis the [19.3] $^2\Pi$ state must correspond to the third or possibly even fourth root of $^2\Pi$ symmetry. The reasonable agreement between the calculated parameters of the $^2\Pi(3)$ state and those measured for the [19.3] $^2\Pi$ state leads us to conclude that the [19.3] $^2\Pi$ state is indeed the third state of $^2\Pi$ symmetry in the LiCa molecule. It must therefore adiabatically correlate to the Li $2s^1$, $^2S$+Ca $4s^13d^1$, $^3D$ separated limit.

The higher energy [22.2] $^2\Pi$ state must then correspond to the fourth root of $^2\Pi$ symmetry, $^2\Pi(4)$, which adiabatically correlates to Li $2s^1$, $^2S$+Ca $4s^13d^1$, $^1D$. The calculated potential curves shown by Allouche and Aubert-Frécon for the $^4\Sigma^+(2)$, $^4\Pi(2)$, and $^4\Delta(1)$ states are all repulsive or only weakly bound, and seem to cross the $^2\Pi(4)$ curve on its repulsive wall.[7] It is therefore possible that the $^2\Pi(4)$ state is predissociated on a time scale that is competitive with photo-ionization. This could explain our difficulty in optimizing

conditions for rotational resolution of the [22.2] $^2\Pi$ ←$X$ $^2\Sigma^+$ band system: under conditions that minimize power broadening resulting from a fast ionization step, predissociation may dominate, leading to a loss of signal intensity.

Turning now to the observed [15.3] $^2\Sigma^+$ state, we note that this state lies more than 5000 cm$^{-1}$ above the calculated energy for the $^2\Sigma^+(2)$ state. It lies only about 1500 cm$^{-1}$ above the $^2\Sigma^+(3)$ state, as calculated in this work, but the measured bond length is 0.4 Å shorter than that calculated for $^2\Sigma^+(3)$ and the measured value of $\Delta G_{1/2}$ is 66% larger than that calculated for $^2\Sigma^+(3)$. On this basis it seems likely that the [15.3] $^2\Sigma^+$ state is the fourth root of $^2\Sigma^+$ symmetry, $^2\Sigma^+(4)$. The $^2\Sigma^+(4)$ state was calculated in the work of Allouche and Aubert-Frécon,[7] and there is substantial agreement between the properties obtained in calculation and those measured (see Table III). Apart from the calculated energy of this state, there is also reasonable agreement between the experimental results and the calculations presented in this paper for the $^2\Sigma^+(4)$ state. On this basis the [15.3] $^2\Sigma^+$ state is assigned as $^2\Sigma^+(4)$, which again correlates adiabatically to Li $2s^1$, $^2S$+Ca $4s^13d^1$, $^3D$.

Overall, it is fair to say that theory and experiment are generally in quite good agreement for the LiCa molecule, provided one considers the theoretical calculations performed at the highest level. The calculated properties of the lower-energy states, not yet experimentally observed, are presumably even more accurate than those of the higher-energy states, which are compared to experiment here.

## I. Expectations for the LiMn and LiZn molecules

The nearly equal sharing of the three valence electrons between the Li and Ca atoms in the ground state of LiCa, leading to Mulliken atomic charges of Li$^{-0.54}$Ca$^{+0.54}$, is not so surprising when one recognizes that Li and Ca have nearly identical electronegativities of 0.97 (Li) and 1.04 (Ca).[26] This is precisely what one would expect if the bonding $1\sigma$ and antibonding $2\sigma$ orbitals were equally shared between the two atoms, which, in turn, would be expected if the electronegativities were identical. In considering LiCa as a model for the interaction between lithium and the $3d^n$ $4s^2$ transition metal atoms Mn and Zn, however, it seems clear that the bond energies of LiMn and LiZn will be greatly reduced as compared to LiCa. In order to form a bond, the $4s$ electrons of the Mn or Zn atom must be partially donated to the lithium atom, leading to unfavorable polarizations of the resulting molecules in the sense Li$^-$Mn$^+$ or Li$^-$Zn$^+$. The greater ionization energies of Mn (7.437 eV)[27] and Zn (9.394 eV)[21] compared to Ca (6.113 eV)[28] imply that electron transfer in this direction cannot occur to the same extent as in LiCa. Electron transfer in the Li$^+$Mn$^-$ or Li$^+$Zn$^-$ direction, on the other hand, is simply not possible because the Mn and Zn atoms lack a suitable acceptor orbital. The net result is even weaker bonding expected in LiMn and LiZn as compared to LiCa. This situation is reminiscent of our previous findings in which AlCa, AlMn, and AlZn all form the ground state of the molecule by placing the single $3p$ electron of the aluminum atom in the $\pi$ orientation, leaving an empty $3p_\sigma$ orbital to accept electron density from the $4s^2$ orbital of Ca,

Mn, or Zn.[2] Although this leads to an increasingly unfavorable charge distribution of $Al^-Ca^+$, $Al^-Mn^+$, and $Al^-Zn^+$, it nevertheless represents the only way a bond can be formed, due to the lack of suitable acceptor orbitals in Ca, Mn, and Zn. The inability of the Li $2s$ electron to readily move to another orbital, however, is a major difference from the case of Al, and suggests that the bond strengths of LiCa, LiMn, and LiZn will be even less that those of AlCa, AlMn, and AlZn, respectively. For LiCa and AlCa calculated bond energies can be compared, and it is indeed true that the bond energy obtained here for LiCa (0.24 eV) is substantially less than that previously obtained for AlCa (0.47 eV),[29] in agreement with this expectation.

## VI. CONCLUSION

A combined experimental and *ab initio* study of LiCa has led to the experimental identification of three band systems, a measurement of the ionization energy, and the theoretical prediction of numerous excited electronic states. It is found that the LiCa molecule has a weakly bound $X\,^2\Sigma^+$ ground state with $r_0 = 3.3796(11)$ Å, $\Delta G_{1/2} = 195.2$ cm$^{-1}$, and $D_e = 0.24$ eV. As in all of the calculated electronic states of LiCa, this state is characterized by substantial electron transfer from Ca to Li, leading to a polarization of the molecule in the sense of $Li^-Ca^+$, with Mulliken charges of $Li^{-0.54}Ca^{+0.54}$. This is in agreement with what might be expected if the bonding $1\sigma$ and antibonding $2\sigma$ orbitals were roughly equally shared between the two atoms.

The low bond energy of this molecule results from the fact that it is composed of two atoms with three $s$ electrons in two $s$ orbitals, resulting in an unfavorable $\sigma^2\sigma^{*1}$ configuration in the ground state of the molecule. In contrast to the weak bond found for this configuration, a strong bond (1.37 eV) is obtained when one of the $\sigma$ electrons is promoted to a $\pi$ orbital, leading to a $\sigma^2\pi^1$ configuration in which all three electrons are in bonding orbitals. This suggests that the related LiZn and LiMn molecules will have low-lying excited states of $^2\Pi$ and $^{5,7}\Pi$ symmetry, correlating to separated atoms in which the lithium atom is excited to its $1s^2 2p^1$, $^2P°$ term.

For the states studied here of $^2\Sigma^+$, $^4\Sigma^-$, $^4\Sigma^+$, $^2\Pi$, and $^4\Pi$ symmetries, the lowest root in every symmetry is always well represented by the Hartree–Fock one-electron configuration, but the second and higher roots are not adequately represented by a single electronic configuration. At least two and sometimes even four or five electronic configurations contribute strongly to the state. As a result these states cannot be described as single-electron promotions from the ground electronic state.

## ACKNOWLEDGMENTS

[1] M. D. Morse, *Advances in Metal and Semiconductor Clusters*, edited by M. A. Duncan (JAI Greenwich, CT., 1993), Vol. 1, p. 83; C. A. Arrington, T. Blume, M. D. Morse, M. Doverståt, and U. Sassenberg, J. Phys. Chem. **98**, 1398 (1994); C. A. Arrington, D. J. Brugh, M. D. Morse, and M. Doverståt, J. Chem. Phys. **102**, 8704 (1995); J. D. Langenberg and M. D. Morse, Chem. Phys. Lett. **239**, 25 (1995).

[2] J. M. Behm and M. D. Morse, Proc. SPIE **2124**, 388 (1994); J. M. Behm and M. D. Morse, J. Chem. Phys. **101**, 6500 (1994).

[3] L. M. Russon, G. K. Rothschopf, and M. D. Morse, J. Chem. Phys. **107**, 1079 (1997).

[4] R. O. Jones, J. Chem. Phys. **72**, 3197 (1980).

[5] D. K. Neumann, D. J. Bernard, and H. H. Michels, Chem. Phys. Lett. **73**, 343 (1980).

[6] C. H. Wu, H. R. Ihle, and K. A. Gingerich, Int. J. Mass Spectrom. Ion Processes **47**, 235 (1983).

[7] A. R. Allouche and M. Aubert-Frécon, Chem. Phys. Lett. **222**, 524 (1994).

[8] L. M. Russon, S. A. Heidecke, M. K. Birke, J. Conceicao, P. B. Armentrout, and M. D. Morse, Chem. Phys. Lett. **204**, 235 (1993); L. M. Russon, S. A. Heidecke, M. K. Birke, J. Conceicao, M. D. Morse, and P. B. Armentrout, J. Chem. Phys. **100**, 4747 (1994).

[9] Similar in design to that described in S. C. O'Brien, Y. Liu, Q. Zhang, J. R. Heath, F. K. Tittel, R. F. Curl, and R. E. Smalley, J. Chem. Phys. **84**, 4074 (1986).

[10] W. C. Wiley and I. H. McLaren, Rev. Sci. Instrum. **26**, 1150 (1955).

[11] S. Gerstenkorn and P. Luc, *Atlas du Spectre d'Absorption de la Molécule d'Iode: 14800–20000* cm$^{-1}$ (CNRS, Paris, 1978); S. Gerstenkorn and P. Luc, Rev. Phys. Appl. **14**, 791 (1979).

[12] D. J. Clouthier and J. Karolczak, Rev. Sci. Instrum. **61**, 1607 (1990).

[13] G. Herzberg, *Molecular Spectra and Molecular Structure I. Spectra of Diatomic Molecules* (Van Nostrand Reinhold, New York, 1950).

[14] See AIP Document No. PAPS JCPSA6-109-002840 for four pages of absolute line positions. Order by PAPS number and journal reference from American Institute of Physics, Physics Auxiliary Publication Service, 500 Sunnyside Boulevard, Woodbury, NY 11797-2999. Fax: 516-576-2223, electronic mail: paps@aip.org. The price is $1.50 for each microfiche (98 pages) or $5.00 for photocopies of up to 30 pages, and $0.15 for each additional page over 30 pages. Airmail additional. Make checks payable to the American Institute of Physics.

[15] H. Lefebvre-Brion and R. W. Field, *Perturbations in the Spectra of Diatomic Molecules* (Academic, Orlando, 1986), p. 125.

[16] B. O. Roos, in *Ab Initio Methods in Quantum Chemistry*, Part II, Advances in Chemical Physics, edited by K. P. Lawley (Wiley, Chichester, 1987), Vol. 69; P.-Å. Malmqvist, A. Rendell, and B. O. Roos, J. Phys. Chem. **94**, 5477 (1990).

[17] P.-O. Widmark, B. J. Persson, and B. O. Roos, Theor. Chim. Acta **79**, 419 (1991).

[18] A. J. Sadlej, Theor. Chim. Acta. **79**, 123 (1991).

[19] K. Anderson, M. P. Fulscher, G. Karlstrom, R. Lindh, P.-Å. Malmqvist, J. Olsen, B. O. Roos, A. Sadlej, University of Lund, Sweden, M. R. A. Blomberg and P. E. M. Siegbahn, University of Stockholm, Sweden, V. Kello, J. Noga, and M. Urban, Comenius University, Slovakia and P.-O. Widmark, IBM, Sweden, MOLCAS-3.

[20] C. E. Moore, Natl. Bur. Stand. Circ. No. 467 (U.S. GPO, Washington, DC, 1949, 1952, 1971).

[21] J. A. Pople, M. Head-Gordon, and K. Raghavachari, J. Chem. Phys. **87**, 5968 (1987).

[22] A. Schäfer, H. Horn, and R. Ahlrichs, J. Chem. Phys. **97**, 2571 (1992).

[23] C. W. Bauschlicher, Jr., S. R. Langhoff, and H. Partridge, J. Chem. Phys. **84**, 901 (1986).

[24] M. J. Frisch, G. W. Trucks, M. Head-Gordon, P. M. W. Gill, M. W. Wong, J. B. Foresman, B. G. Johnson, H. B. Schlegel, M. A. Robb, E. S. Reploge, R. Gomperts, J. L. Anders, K. Raghavachari, J. S. Binkley, C. Gonzales, R. L. Martin, D. J. Fox, D. J. Defrees, J. Baker, J. J. P. Stewart, and J. A. Pople, GAUSSIAN 92, Revision C, Gaussian Inc., Pittsburgh, PA, 1992.

[25] E. Ilyabaev and U. Kaldor, J. Chem. Phys. **98**, 7126 (1993).

[26] A. L. Allred and E. G. Rochow, J. Inorg. Nucl. Chem. **5**, 264 (1958).

[27] C. Corliss and J. Sugar, J. Phys. Chem. Ref. Data **6**, 1253 (1977).

[28] J. Sugar and C. Corliss, J. Phys. Chem. Ref. Data **8**, 865 (1979).

[29] J. M. Behm, M. D. Morse, A. I. Boldyrev, and J. Simons, J. Chem. Phys. **101**, 5441 (1994).